

Charged Higgs Effects on Exclusive Semi-tauonic B Decays

M. Tanaka*

Theory Group, KEK, Tsukuba, Ibaraki 305, Japan

Abstract

We study effects of charged Higgs boson exchange in the B semileptonic decays $\bar{B} \rightarrow D^{(*)}\tau\bar{\nu}_\tau$. Both branching ratio and τ polarization are examined. We use the recent experimental data on semileptonic B decays and the heavy quark effective theory in order to reduce theoretical uncertainty in the hadronic form factors. Theoretical uncertainty in the branching ratio is found to be rather small and that in the τ polarization is almost negligible. Their measurements will give nontrivial constraints on the charged Higgs sector.

To be published in Zeitschrift für Physik C.

*Electronic address: minoru@theory.kek.jp

The evidence for top quarks [1] leaves the Higgs sector as the only missing part of the standard model (SM). In the minimal SM, we have one Higgs doublet, which gives a neutral scalar particle as a physical state. An extension of the Higgs sector is an interesting possibility for new physics beyond the SM. One of the most attractive possibilities is the supersymmetric extension of the SM [2]. In the minimal supersymmetric SM, we have to introduce two Higgs doublets in order to cancel the anomaly and to give the fermions masses. Another important possibility is CP violation in the Higgs sector [3,4]. It is known that CP can be broken in the Higgs sector if we have two or more Higgs doublets. Since the existence of one or more charged Higgs bosons is an inevitable consequence of the multi-Higgs-doublet extensions of the SM, the search for their effects is one of the key points in the quest for new physics.

The most stringent experimental bound on the charged Higgs boson mass at present is $m_H \gtrsim 260\text{GeV}$, given by the measurement of the inclusive radiative b quark decay $b \rightarrow s\gamma$ [5]. This bound was found for the two-Higgs-doublet model of the ‘‘SUSY-type’’ Higgs couplings to fermions, called Model II [6]. Since this process takes place via 1-loop diagrams, the bound may be changed depending on details of the model considered. If the model contains new particles other than the charged Higgs boson which contribute to the $b \rightarrow s\gamma$ process, the above lower bound may be modified. This is indeed the case in the minimal supersymmetric SM [7]. From this point of view, it is worthwhile to investigate charged Higgs boson effects in tree level processes which are less dependent on the other sectors of the multi-Higgs-doublet models.

In this paper, we study effects of the charged Higgs boson on the branching ratio and the τ polarization of the processes $\bar{B} \rightarrow D^{(*)}\tau\bar{\nu}_\tau$. These processes are expected to be much more sensitive to the charged Higgs sector than the semileptonic K decay processes because the Higgs couplings to fermions are proportional to the fermion mass. The 1% level branching ratio of these modes expected in the SM will give of order 10^6 semi-tauonic B decay events at the planned B factories.

In N -Higgs-doublet models, we have $N - 1$ physical charged Higgs bosons. Their cou-

plings to quarks and leptons are described by the following interaction Lagrangian [8]:

$$\mathcal{L}_H = (2\sqrt{2}G_F)^{1/2} \sum_{i=1}^{N-1} \left[X_i \bar{U}_L V_{KM} M_D D_R + Y_i \bar{U}_R M_U V_{KM} D_L + Z_i \bar{N}_L M_E E_R \right] H_i^+ + \text{h.c.} . \quad (1)$$

Here H_i^\pm is the i -th lightest physical charged Higgs boson,

$$U_{L(R)} = (u, c, t)_{L(R)}^T, \quad D_{L(R)} = (d, s, b)_{L(R)}^T, \quad N_L = (\nu_e, \nu_\mu, \nu_\tau)_L^T, \quad E_R = (e, \mu, \tau)_R^T, \quad (2)$$

$$M_U = \text{diag.}(m_u, m_c, m_t), \quad M_D = \text{diag.}(m_d, m_s, m_b), \quad M_E = \text{diag.}(m_e, m_\mu, m_\tau), \quad (3)$$

represent the quark and lepton fields and their masses respectively, and V_{KM} is the Kobayashi-Maskawa matrix. Note that the KM matrix which appears in the charged current mixing appears in the above Lagrangian. This is a consequence of the natural flavor conservation [9] which we implicitly assumed in Eq. (1) in order to suppress flavor changing neutral Higgs interactions.

In the case of $N \geq 3$, the coefficients X_i, Y_i, Z_i can be complex, while they are real when $N = 2$. In particular they are real in Model II of two-Higgs-doublets or in the minimal supersymmetric SM, and can be written as [6]

$$X_1 = Z_1 = \tan \beta, \quad Y_1 = \cot \beta, \quad (4)$$

where $\tan \beta = v_u/v_d$ is the ratio of the vacuum expectation values of the two Higgs fields.

Given the above Lagrangian in Eq. (1) and the standard charged current Lagrangian, we can evaluate effects of the charged Higgs boson exchange in $\bar{B} \rightarrow M\tau\bar{\nu}_\tau$ processes for $M = D$ or D^* . We adopt a helicity amplitude formalism since it is convenient for calculating τ polarizations. We follow the convention in Refs. [10] and [11].

The W boson exchange amplitude is given by

$$\mathcal{M}_{\lambda_M}^{\lambda_\tau}(q^2, x)_W = \frac{G_F}{\sqrt{2}} V_{cb} \frac{M_W^2}{M_W^2 - q^2} \sum_{\lambda_W} \eta_{\lambda_W} L_{\lambda_W}^{\lambda_\tau} H_{\lambda_W}^{\lambda_M}, \quad (5)$$

where $\lambda_M = \pm, 0$ denote three possible D^* helicity states, $\lambda_M = s$ stands for the D mode, and $\lambda_\tau = \pm$ is the τ helicity. The invariant mass squared of the leptonic system is q^2 , and

$x = p_\tau \cdot p_B / m_B^2$ is the τ energy divided by the B meson mass in the \bar{B} meson rest frame. The virtual W helicity is denoted by $\lambda_W = \pm, 0, s$, and the metric factor η_{λ_W} is given by $\eta_{\pm,0} = 1$ and $\eta_s = (q^2 - M_W^2) / M_W^2$. The hadronic and leptonic amplitudes which describe the processes $\bar{B} \rightarrow MW^*$ and $W^* \rightarrow \tau \bar{\nu}_\tau$ are defined respectively by

$$H_{\lambda_W}^{\lambda_M}(q^2) \equiv \epsilon_\mu^*(\lambda_W) \langle M(p_M, \lambda_M) | \bar{c} \gamma^\mu (1 - \gamma_5) b | \bar{B}(p_B) \rangle, \quad (6)$$

and

$$L_{\lambda_W}^{\lambda_\tau}(q^2, x) \equiv \epsilon_\mu(\lambda_W) \langle \tau(p_\tau, \lambda_\tau) \bar{\nu}_\tau(p_\nu) | \bar{\tau} \gamma^\mu (1 - \gamma_5) \nu_\tau | 0 \rangle, \quad (7)$$

where $\epsilon_\mu(\lambda_W)$ is the polarization vector of the virtual W boson. Note that the leptonic amplitude $L_{\lambda_W}^{\lambda_\tau}$ depends on the frame in which the τ helicity is defined. $L_{\lambda_W}^{\lambda_\tau}$ with the τ helicity defined in the virtual W rest frame is given in Ref. [10] and the one with the τ helicity defined in the initial \bar{B} rest frame is given in Ref. [11]. The hadronic amplitude is also given in Ref. [10].

The amplitude of the charged Higgs exchange can be written as

$$\mathcal{M}_{\lambda_M}^{\lambda_\tau}(q^2, x)_H = \frac{G_F}{\sqrt{2}} V_{cb} \sum_i L^{\lambda_\tau} \left[X_i Z_i^* \frac{m_b m_\tau}{M_{H_i}^2 - q^2} H_R^{\lambda_M} + Y_i Z_i^* \frac{m_c m_\tau}{M_{H_i}^2 - q^2} H_L^{\lambda_M} \right], \quad (8)$$

where

$$H_{R,L}^{\lambda_M}(q^2) \equiv 2 \langle M(p_M, \lambda_M) | \bar{c} P_{R,L} b | \bar{B}(p_B) \rangle, \quad P_R = \frac{1 + \gamma_5}{2}, \quad P_L = \frac{1 - \gamma_5}{2}, \quad (9)$$

$$L^{\lambda_\tau}(q^2, x) \equiv \langle \tau(p_\tau, \lambda_\tau) \bar{\nu}_\tau(p_\nu) | \bar{\tau} (1 - \gamma_5) \nu_\tau | 0 \rangle. \quad (10)$$

Using the equations of motion, the hadronic and leptonic amplitudes of charged Higgs exchange are related to those of W exchange with scalar W^* polarization ($\lambda_W = s$):

$$H_{R,L}^s = \frac{\sqrt{q^2}}{m_b - m_c} H_s^s, \quad H_R^\pm = 0, \quad H_R^0 = \frac{\sqrt{q^2}}{m_b + m_c} H_s^0, \quad H_L^{\pm,0} = -H_R^{\pm,0}, \quad (11)$$

$$L^{\lambda_\tau} = \frac{\sqrt{q^2}}{m_\tau} L_s^{\lambda_\tau}. \quad (12)$$

As can be seen in Eq. (11), the Higgs exchange does not contribute to the decay into transversely polarized D^* meson ($\lambda_M = \pm$) because of angular momentum conservation. Therefore, we study charged Higgs boson effects in \bar{B} decays into D mesons ($\lambda_M = s$) and those into longitudinally polarized D^* mesons ($\lambda_M = 0$) in the \bar{B} rest frame.

Using the helicity amplitudes of Eqs. (5) and (8), it is straightforward to calculate the differential decay rate¹:

$$d\Gamma_{\lambda_M} = \frac{1}{2m_B} \sum_{\lambda_\tau} |\mathcal{M}_{\lambda_M}^{\lambda_\tau}|^2 d\Phi_3, \quad (13)$$

where $\mathcal{M}_{\lambda_M}^{\lambda_\tau} = \mathcal{M}_{\lambda_M}^{\lambda_\tau}(q^2, x)_W + \mathcal{M}_{\lambda_M}^{\lambda_\tau}(q^2, x)_H$, and $d\Phi_3 = dq^2 dx/64\pi^3$ is the three-body phase space. Also, τ polarizations can be calculated conveniently with the helicity amplitudes. Let us consider the decay rate with a definite τ spin direction. It can be written as

$$d\Gamma_{\lambda_M}(\mathbf{s}) = \frac{1}{2} \left[d\Gamma_{\lambda_M} + (d\Gamma_{\lambda_M}^L \mathbf{e}_L + d\Gamma_{\lambda_M}^\perp \mathbf{e}_\perp + d\Gamma_{\lambda_M}^T \mathbf{e}_T) \cdot \mathbf{s} \right], \quad (14)$$

where \mathbf{s} is the unit vector which points toward the τ spin direction in the τ rest frame, and the basis vectors are defined as $\mathbf{e}_L \equiv \mathbf{p}_\tau/|\mathbf{p}_\tau|$, $\mathbf{e}_T \equiv \mathbf{p}_M \times \mathbf{p}_\tau/|\mathbf{p}_M \times \mathbf{p}_\tau|$, and $\mathbf{e}_\perp \equiv \mathbf{e}_T \times \mathbf{e}_L$, with the convention that the angle from \mathbf{p}_M to \mathbf{p}_τ lies between 0 and π . The situation is depicted in Fig. 1. These definitions can be used both in the virtual W (or Higgs) rest frame and in the \bar{B} rest frame. The components of the spin-dependent part of the decay rate in Eq. (14) are given in terms of the helicity amplitudes as

$$d\Gamma_{\lambda_M}^L = \frac{1}{2m_B} \left(|\mathcal{M}_{\lambda_M}^+|^2 - |\mathcal{M}_{\lambda_M}^-|^2 \right) d\Phi_3, \quad (15)$$

$$d\Gamma_{\lambda_M}^\perp = \frac{1}{m_B} \text{Re} \left(\mathcal{M}_{\lambda_M}^{+*} \mathcal{M}_{\lambda_M}^- \right) d\Phi_3, \quad (16)$$

$$d\Gamma_{\lambda_M}^T = \frac{1}{m_B} \text{Im} \left(\mathcal{M}_{\lambda_M}^{+*} \mathcal{M}_{\lambda_M}^- \right) d\Phi_3. \quad (17)$$

¹The decay distributions of the charge conjugate processes ($B \rightarrow \bar{M}\tau^+\nu_\tau$ with $M = \bar{D}, \bar{D}^*$) are obtained by taking complex conjugate of all the couplings.

From Eq. (14), the possible three τ polarizations are defined by

$$P_L \equiv \frac{d\Gamma(\mathbf{e}_L) - d\Gamma(-\mathbf{e}_L)}{d\Gamma(\mathbf{e}_L) + d\Gamma(-\mathbf{e}_L)} = \frac{d\Gamma^L}{d\Gamma} , \quad (18)$$

$$P_\perp \equiv \frac{d\Gamma(\mathbf{e}_\perp) - d\Gamma(-\mathbf{e}_\perp)}{d\Gamma(\mathbf{e}_\perp) + d\Gamma(-\mathbf{e}_\perp)} = \frac{d\Gamma^\perp}{d\Gamma} , \quad (19)$$

$$P_T \equiv \frac{d\Gamma(\mathbf{e}_T) - d\Gamma(-\mathbf{e}_T)}{d\Gamma(\mathbf{e}_T) + d\Gamma(-\mathbf{e}_T)} = \frac{d\Gamma^T}{d\Gamma} , \quad (20)$$

where we omit the common helicity index λ_M . Note that $P_L^2 + P_\perp^2 + P_T^2 = 1$ at an arbitrary kinematical configuration because of the definite neutrino helicity. The longitudinal polarization (P_L) and the perpendicular polarization (P_\perp) depend on the frame in which the τ helicity is defined. On the other hand, the transverse polarization (P_T) is frame-independent. It is well-known that the transverse polarization is a T-violating quantity as long as the final state interaction can be ignored. The T- or CP-violating nature of the transverse polarization can be seen in Eq. (17) since all the tree-level amplitudes of Eqs. (5) and (8) are chosen to be real in the CP-conserving limit in our convention.

In order to find numerical predictions, the hadronic transition form factors are needed. In Ref. [10], the following set of hadronic form factors are employed and the hadronic amplitude $H_{\lambda_W}^{\lambda_M}$ in Eq. (6) is given in terms of them:

$$\langle D(p_M) | \bar{c}\gamma^\mu b | \bar{B}(p_B) \rangle = f_+(q^2)(p_B + p_M)^\mu + f_-(q^2)(p_B - p_M)^\mu , \quad (21)$$

$$\langle D^*(p_M, \lambda_M) | \bar{c}\gamma^\mu b | \bar{B}(p_B) \rangle = if_1(q^2)\epsilon^{\mu\nu\rho\sigma}\epsilon_{M\nu}^*(p_B + p_M)_\rho(p_B - p_M)_\sigma , \quad (22)$$

$$\langle D^*(p_M, \lambda_M) | \bar{c}\gamma^\mu\gamma_5 b | \bar{B}(p_B) \rangle = f_2(q^2)\epsilon_M^{*\mu} + \epsilon_M^* \cdot p_B \left\{ f_3(q^2)(p_B + p_M)^\mu + f_4(q^2)(p_B - p_M)^\mu \right\} , \quad (23)$$

where $\epsilon_M = \epsilon_M(p_M, \lambda_M)$ is the polarization vector of the D^* meson. In the following, however, we adopt a different set of form factors which is more convenient to incorporate the results of the heavy quark effective theory. We use the following form factors [12]:

$$\langle D(v') | \bar{c} \gamma^\mu b | \bar{B}(v) \rangle = \sqrt{m_B m_M} [\xi_+(y)(v + v')^\mu + \xi_-(y)(v - v')^\mu] , \quad (24)$$

$$\langle D^*(v', \lambda_M) | \bar{c} \gamma^\mu b | \bar{B}(v) \rangle = i \sqrt{m_B m_M} \xi_V(y) \epsilon^{\mu\nu\rho\sigma} \epsilon_{M\nu}^* v'_\rho v_\sigma , \quad (25)$$

$$\langle D^*(v', \lambda_M) | \bar{c} \gamma^\mu \gamma_5 b | \bar{B}(v) \rangle = \sqrt{m_B m_M} [\xi_{A_1}(y)(1 + y) \epsilon_M^{*\mu} - \xi_{A_2}(y) \epsilon_M^* \cdot v v^\mu - \xi_{A_3}(y) \epsilon_M^* \cdot v v'^\mu] , \quad (26)$$

where $v = p_B/m_B$ and $v' = p_M/m_M$ are the four-velocities of the \bar{B} and $M(= D, D^*)$ mesons respectively, and $y \equiv v \cdot v' = (m_B^2 + m_M^2 - q^2)/(2m_B m_M)$. The form factors in Eqs. (21)~(23) can be written in terms of the form factors in Eqs. (24)~(26):

$$f_\pm = \pm \frac{1}{2\sqrt{r}} [(1 \pm r)\xi_+ - (1 \mp r)\xi_-] , \quad (27)$$

$$f_1 = \frac{1}{2m_B \sqrt{r}} \xi_V , \quad f_2 = m_B \left(\sqrt{r} + \frac{p_B \cdot p_M}{m_B^2 \sqrt{r}} \right) \xi_{A_1} , \quad f_{3,4} = -\frac{1}{2m_B} \left(\sqrt{r} \xi_{A_2} \pm \frac{1}{\sqrt{r}} \xi_{A_3} \right) , \quad (28)$$

where $r = m_M/m_B$ and we omitted the arguments of the f 's and ξ 's.

In the heavy quark limit and in the leading logarithmic approximation (LLA), we have [13,14]

$$\xi_+ = \xi_V = \xi_{A_1} = \xi_{A_3} \equiv C \xi , \quad \xi_- = \xi_{A_2} = 0 , \quad (29)$$

where $\xi(1) = 1$ and C denotes the QCD correction factor in the LLA². We assume the following form of the universal form factor³,

$$\xi(y) = \left(\frac{2}{1+y} \right)^{2\rho^2} , \quad (30)$$

²The factor C drops out in our results.

³The following results in this paper are not affected significantly by adopting alternative forms such as those used in Ref. [15]

and determine the slope parameter ρ from the experimental data of semileptonic B decays [16]. As a result, we obtain

$$\rho = 1.08 \pm 0.11 , \quad (31)$$

with $\chi^2_{min}/d.o.f. = 0.48$. Eq. (31) gives the uncertainty of the predictions in the approximation of Eqs. (29) and (30).

In our numerical analysis, we consider only the effects of the lightest charged Higgs boson exchange. Other charged Higgs bosons (if they exist) are assumed to be too heavy to give significant contributions. Moreover, we concentrate on the case of the Model II Higgs couplings as shown in Eq. (4). So, the strength of the charged Higgs couplings to fermions are determined by $\tan \beta$ only.

We use $m_b = 4.8\text{GeV}$, $m_c = 1.4\text{GeV}$, and $m_\tau = 1.78\text{GeV}$, and we do not consider the uncertainty in the quark masses, because its effect appears mostly through the combination $m_b m_\tau \tan^2 \beta / M_H^2$ and a variation in m_b can be absorbed by changing $\tan \beta$ or the charged Higgs boson mass M_H .

Our predictions for the branching ratio are shown in Figs. 2 and 3. In Figs. 2(a) and 3(a), we show the decay rate of the process $\bar{B} \rightarrow D^{(*)} \tau \bar{\nu}_\tau$ in the presence of the charged Higgs boson exchange, normalized to the rate of $\bar{B} \rightarrow D^{(*)} \mu \bar{\nu}_\mu$ in the SM, against the charged Higgs mass for several values of $\tan \beta$. The shaded regions correspond to the predictions in the approximation of Eqs. (29) and (30) within the uncertainty of Eq. (31). In Figs. 2(b) and 3(b), we also show the decay rate normalized to $\tilde{\Gamma}$, the decay rate of $\bar{B} \rightarrow D^{(*)} \mu \bar{\nu}_\mu$ in the SM, but integrated in the same q^2 region as the τ mode, *i.e.* $m_\tau^2 \leq q^2 \leq (m_B - m_M)^2$. As seen in Figs. 2 and 3, this restriction in the q^2 range decreases the uncertainty in the hadronic form factors and improve the sensitivity to the charged Higgs sector. The theoretical sensitivity to the charged Higgs sector can be represented by the minimum value of $R \equiv M_W \tan \beta / M_H$ which can be detected in an ideal experiment. From Fig. 2(b), we expect the theoretical reach of $R \sim 6$ with the uncertainty of Eq. (31). As can be seen in Fig. 3, the longitudinal D^* (D_L^*) mode is less sensitive to the charged Higgs boson exchange because of the angular

momentum barrier. Actually, the hadronic amplitude $H_s^0(q^2)$ vanishes as $q^2 \rightarrow (m_B - m_M)^2$.

In order to get an idea on the size of the $1/m_{b,c}$ correction and the non-LLA QCD correction which violate the relation among the form factors in Eq. (29), we employ the estimation of these corrections by Neubert [17]. In Ref. [17] both the $1/m_{b,c}$ correction as estimated by the QCD sum rule and the perturbative QCD correction beyond the LLA are given. The form factors in Eqs. (24)~(26) are then written as

$$\xi_i(y) = [\alpha_i + \beta_i(y) + \gamma_i(y)] \xi(y), \quad i = +, -, V, A_1, A_2, A_3, \quad (32)$$

where $\alpha_+ = \alpha_V = \alpha_{A_1} = \alpha_{A_3} = 1$, $\alpha_- = \alpha_{A_2} = 0$, $\beta_i(y)$ represents the perturbative QCD correction, and $\gamma_i(y)$ is the $1/m_{b,c}$ correction. The functions β_i 's and γ_i 's are given in Ref. [17]. Assuming the form of $\xi(y)$ in Eq. (30) again, we obtain the following range of the slope parameter from the experimental data [16]:

$$\rho = 1.23 \pm 0.09, \quad (33)$$

with $\chi_{min}^2/d.o.f. = 0.55$.

The results on the decay rate by using Eq. (32) and the central value of Eq. (33), *i.e.* $\rho = 1.23$, are shown in Figs. 2 and 3 by dashed lines. The magnitude of the uncertainty from the range of the parameter ρ in Eq. (33) is roughly as the same as in the leading order approximation of Eqs. (29) ~ (31). Fig. 2 shows that the non-leading corrections are not the major uncertainty in the \bar{B} to D mode, and the theoretical reach of $R \sim 6$ for the D mode remains valid. On the other hand, as can be seen from Fig. 3, the non-leading corrections can be as large as the uncertainty in the slope parameter of Eq. (33) for the D_L^* mode. In future, the non-leading corrections may become dominant uncertainties in both the D and D_L^* modes if the ranges of Eqs. (31) and (33) are reduced enough by detailed studies of the semileptonic B decays at B factories.

As for the τ polarizations, we can calculate any of their distributions by using Eqs. (13) and (15)~(20) given the helicity amplitudes. For the couplings of Eq. (4), we obtain $P_T = 0$, and $P_L^2 + P_\perp^2 = 1$ at any phase space point (q^2, x) . However, for simplicity, we concentrate

on the longitudinal polarization P_L integrated over the whole phase space separately in the numerator and the denominator of Eq. (18). Note that $P_L^2 + P_\perp^2 \neq 1$ after this integration. In the following, we consider two of the possible frames in which the τ helicity is defined, the virtual $W(H)$ rest frame and the \bar{B} rest frame. The longitudinal τ polarization in the former frame is denoted by $P_L(W^*)$, and in the latter frame by $P_L(B)$.

Our numerical results on $P_L(W^*)$ and $P_L(B)$ are given in Figs. 4 and 5. Fig. 4(a) and (b) show the $P_L(W^*)$ and the $P_L(B)$ respectively in the D mode. Fig. 5(a) and (b) show the same quantities in the D_L^* mode. The values in the leading order approximation of Eqs. (29) and (30) with the uncertainty due to the range of ρ in Eq. (31) are again shown by the shaded region. The uncertainty in the prediction is found to be much smaller than that in the branching ratio; it is almost negligible except for $P_L(B)$ in the D mode. The predictions with the non-leading corrections of Eq. (32) for the central value of Eq. (33) are also shown by dashed lines. The non-leading corrections can be regarded as the major uncertainty in the calculations of these polarizations except for $P_L(B)$ in the D mode.

From Fig. 4(a), we expect the best possible theoretical reach of $R \sim 4.5$ among the calculations in this paper, regarding the difference between the center line of the shaded region which shrinks to almost a line and the dashed line as possible theoretical uncertainties. However, this estimation of the theoretical reach is rather ambiguous because it heavily relies on the estimation of the non-leading corrections in Ref. [17]. On the other hand, as expected, the D_L^* mode is less sensitive to the charged Higgs boson exchange in these polarizations too, see Fig. 5.

The above results on the sensitivity of the branching ratio and the τ polarizations to the charged Higgs boson effects in the exclusive semi-tauonic B decays should be compared with those in the inclusive semi-tauonic B decay. The inclusive decay has been studied in Ref. [18], which finds the sensitivity of $R \sim 32$ for the branching ratio, and $R \sim 20$ for the

τ polarization⁴, despite the fact that the uncertainties in the inclusive study of Ref. [18] seem to be slightly smaller than those in the exclusive study of the present paper. These less sensitive results are understood as the above-explained insensitivity of the D^* mode which gives a large portion of the inclusive decay and cannot be separated in the inclusive study. In other words, the D^* modes dilute the effects of the charged Higgs boson exchange in the inclusive decay. On the other hand, in the exclusive study, we can select out the sensitive D mode. Therefore, measurements of the branching ratio and the τ polarizations for $\bar{B} \rightarrow D\tau\bar{\nu}_\tau$ mode may give the best bound on the charged Higgs boson exchange at the tree level.

Finally, we comment on reconstruction of the τ momentum. Reconstruction of the τ momentum is desirable in several measurements discussed above, in particular it is necessary to measure x and q^2 distributions. Even if we know the momenta p_B , p_M , and p_h in the decay process $\bar{B} \rightarrow M\tau\bar{\nu}_\tau$ followed by $\tau \rightarrow \text{hadrons}(h) + \nu_\tau$, the τ momentum cannot be reconstructed because of two missing neutrinos. In this case, the τ momentum is parametrized by its azimuthal angle in the virtual $W(H)$ rest frame in which \mathbf{p}_h points toward the positive z direction. Improvements in vertex detector technology can improve the situation. Measurements of several quantities in semi-tauonic B decays should be improved significantly by systematically taking into account the vertex information. In principle, by using the knowledge about the tracks originating from M and τ , we can measure the impact parameter between the flight lines of M and h . If the position of the \bar{B} decay vertex or the τ decay vertex is known in addition to this impact parameter, we can obtain the τ momentum by determining the azimuthal angle mentioned above. However, there remains a two-fold ambiguity in general. To disentangle this ambiguity, both the \bar{B} decay vertex and the τ decay vertex should be known. In principle, the \bar{B} decay vertex can be measured when the beam axis is well-known or when \bar{B} decays into D^* . The τ decay vertex can be measured

⁴In Ref. [18], the longitudinal τ polarization in the \bar{B} rest frame is discussed.

in the three-prong decays.

The author would like to thank K. Hagiwara for his careful reading of the manuscript and valuable discussions. He also thanks Y. Kuno for useful discussions and B. Bullock for his reading of the manuscript.

REFERENCES

- [1] CDF Collaboration (F. Abe *et al.*), Phys. Rev. **D50**, 2966 (1994).
- [2] For a recent review, *e.g.*, H. E. Haber and G. L. Kane, Phys. Rep. **117**, 75 (1985).
- [3] T.D. Lee, Phys. Rev. **D8**, 1226 (1973); Phys. Rep. **9C**, 143 (1974).
- [4] S. Weinberg, Phys. Rev. Lett. **37**, 657 (1976).
- [5] CLEO Collaboration (B. Barish *et al.*), CLEO CONF 94-1, 1994 (unpublished).
- [6] J.F. Gunion, H.E. Haber, G.L. Kane, and S. Dawson, *The Higgs Hunter's Guide* (Addison-Wesley Publishing Company, 1990), and references therein.
- [7] R. Barbieri and G.F. Giudice, Phys. Lett. **B309**, 86 (1993).
- [8] C. Albright, J. Smith, and S.-H. Tye, Phys. Rev. **D21**, 711 (1980).
- [9] S.L. Glashow and S. Weinberg, Phys. Rev. **D15**, 1958 (1977).
- [10] K. Hagiwara, A.D. Martin, and M.F. Wade, Nucl. Phys. **B327**, 569 (1989).
- [11] K. Hagiwara, A.D. Martin, and M.F. Wade, Z. Phys. **C46**, 299 (1990).
- [12] M. Neubert, Phys. Lett. **B264**, 455 (1991).
- [13] M.B. Voloshin and M.A. Shifman, Yad. Fiz. **45**, 463 (1987) [Sov. J. Nucl. Phys. **45**, 292 (1987)]; H.D. Politzer and M.B. Wise, Phys. Lett **B206**, 681 (1988); Phys. Lett **B208**, 504 (1988).
- [14] N. Isgur and M.B. Wise, Phys. Lett **B232**, 113 (1989); Phys. Lett **B237**, 527 (1990).
- [15] ARGUS Collaboration (H. Albrecht *et al.*), Z. Phys. **C57**, 533 (1993).
- [16] CLEO Collaboration (B. Barish *et al.*), CLNS 94/1285, 1994 (unpublished).
- [17] M. Neubert, Phys. Rev. **D46**, 3914 (1992).
- [18] Y. Grossman and Z. Ligeti, Phys. Lett. **B332**, 373 (1994).

FIGURES

FIG. 1. Kinematics and definition of the basis vectors of τ polarization.

FIG. 2. The branching ratios for the D mode: The shaded regions show the predictions within the uncertainty in ρ (Eq. (31)) in the approximation of Eqs. (29) and (30), and the dashed lines are the predictions with the non-leading corrections of Eq. (32) for the central value of Eq. (33). (a) The decay rate normalized to that of $\bar{B} \rightarrow D\mu\bar{\nu}_\mu$ in the SM: (b) The same as (a) except that the denominator is integrated over the region $m_\tau^2 \leq q^2 \leq (m_B - m_M)^2$.

FIG. 3. The branching ratios for the D_L^* mode: The same as Fig. 2.

FIG. 4. The τ polarizations for the D mode: The uncertainties are shown in the same way as Figs. 2 and 3. The longitudinal τ polarizations, (a) in the virtual $W(H)$ rest frame, and (b) in the \bar{B} rest frame are shown.

FIG. 5. The τ polarizations for the D_L^* mode: The same as Fig. 4.

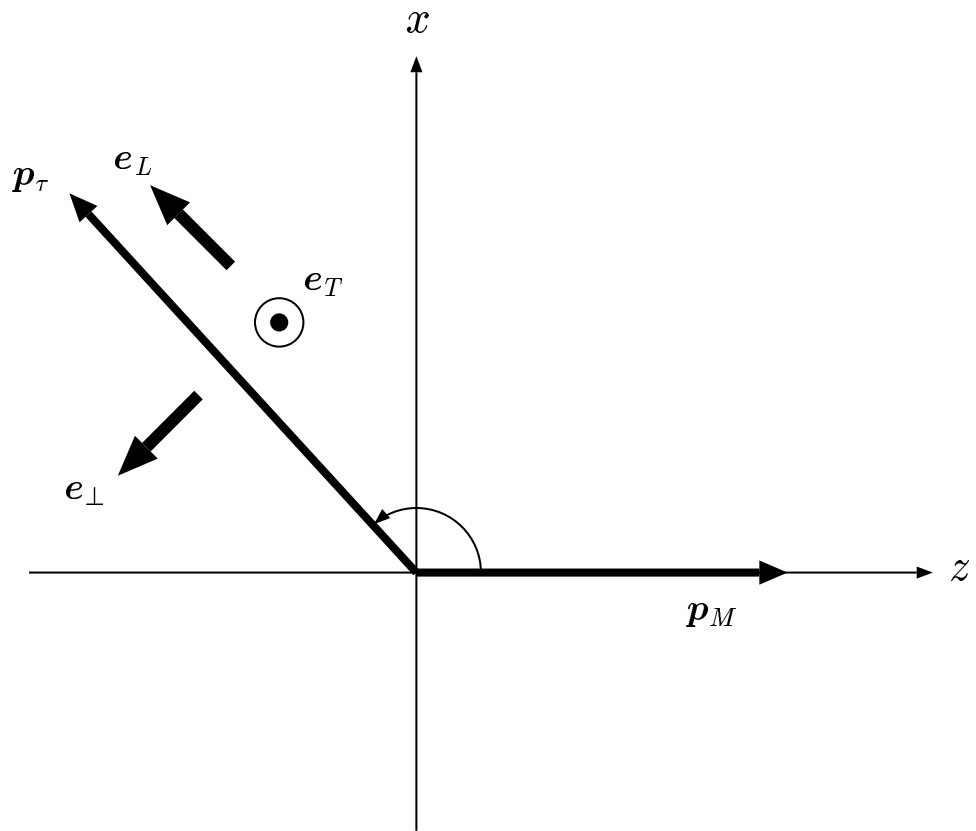


Fig. 1

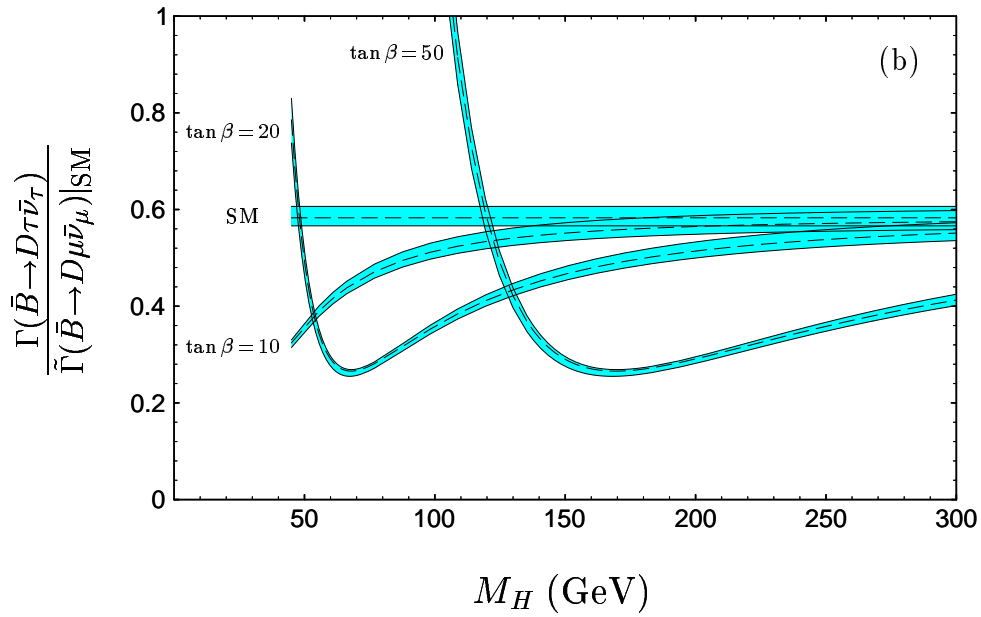
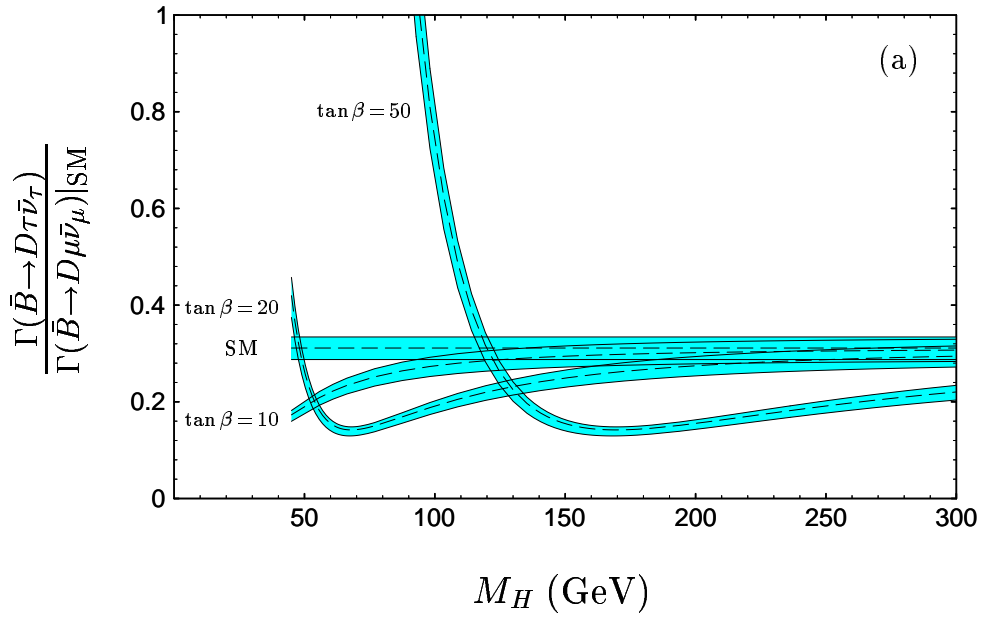


Fig. 2

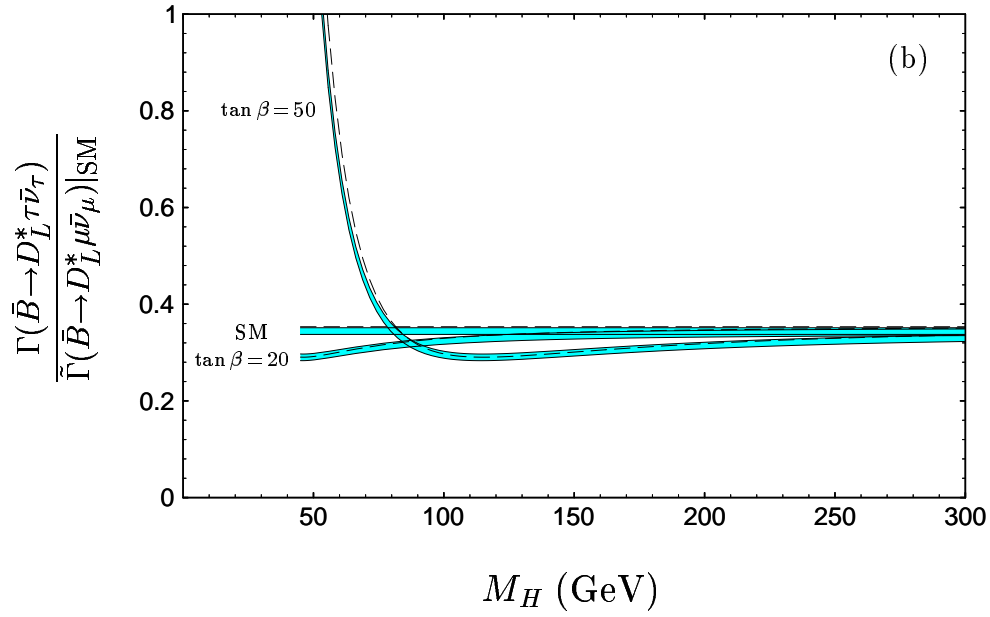
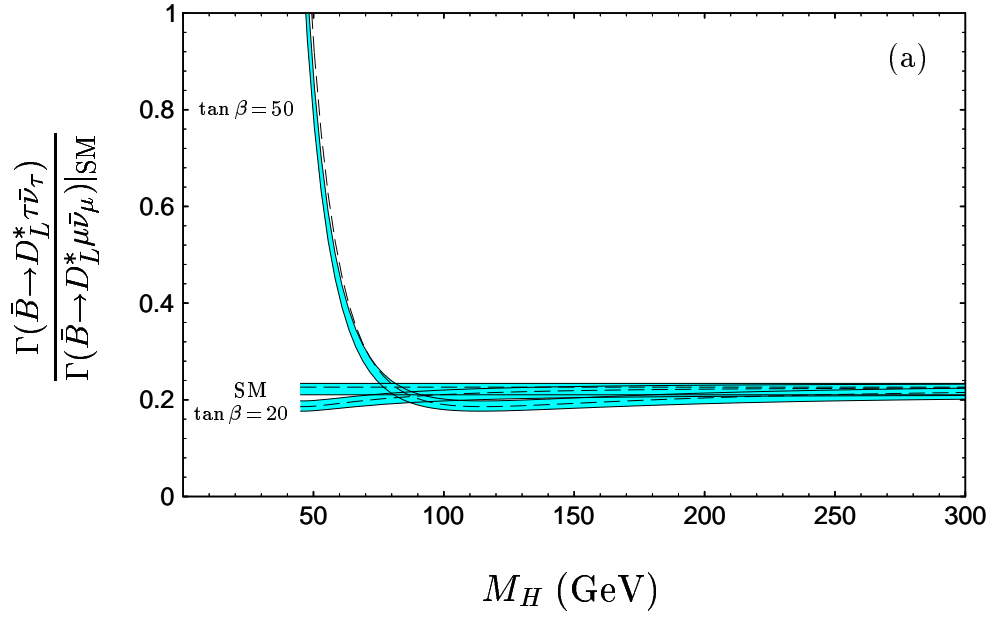


Fig. 3

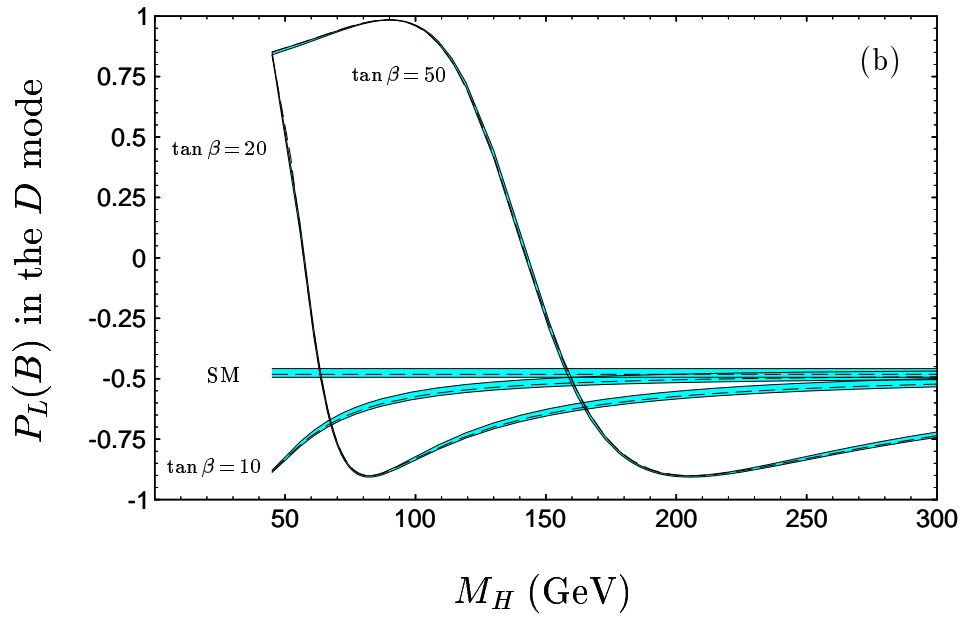
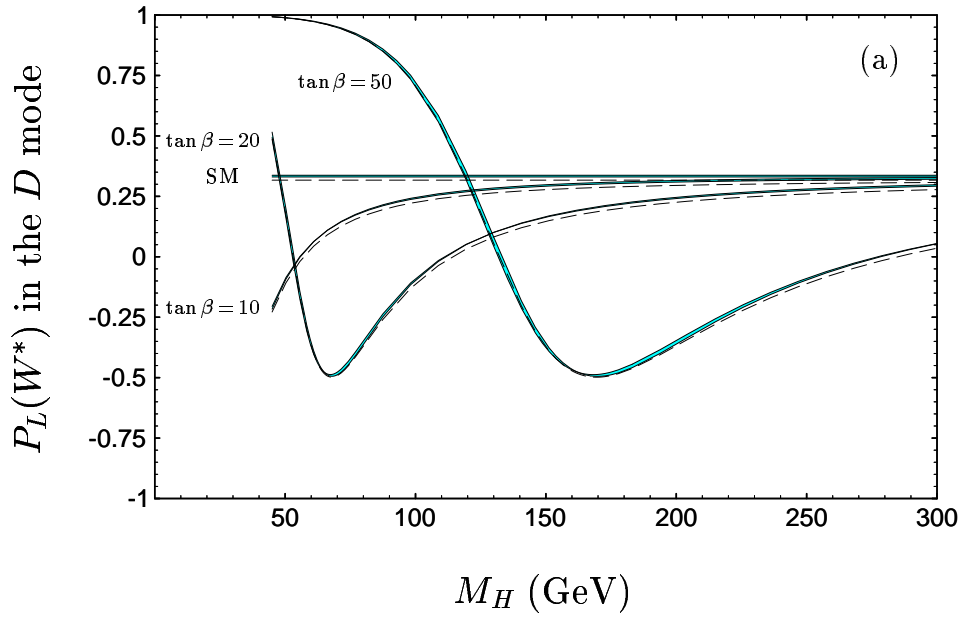


Fig. 4

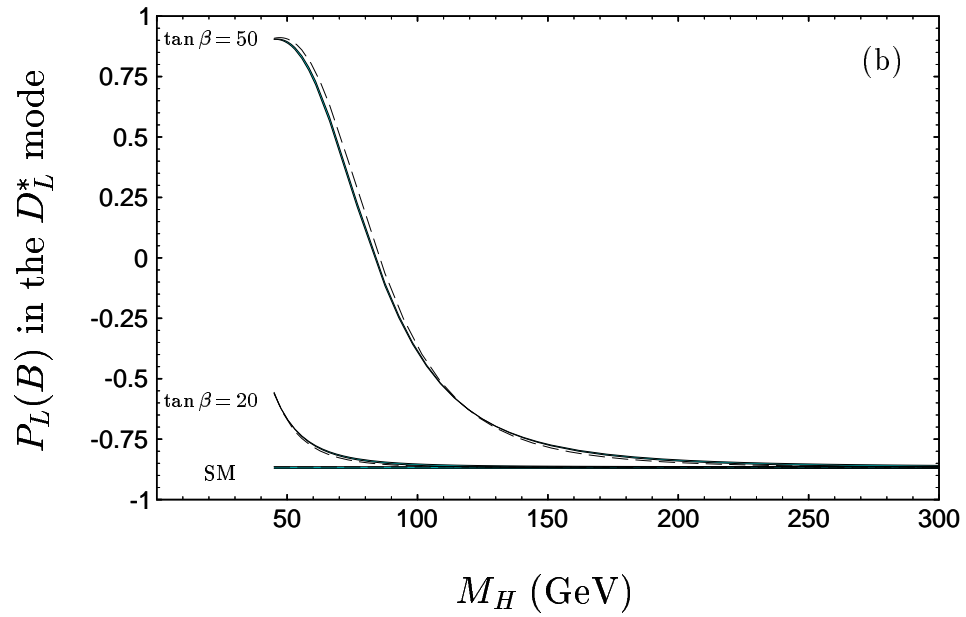
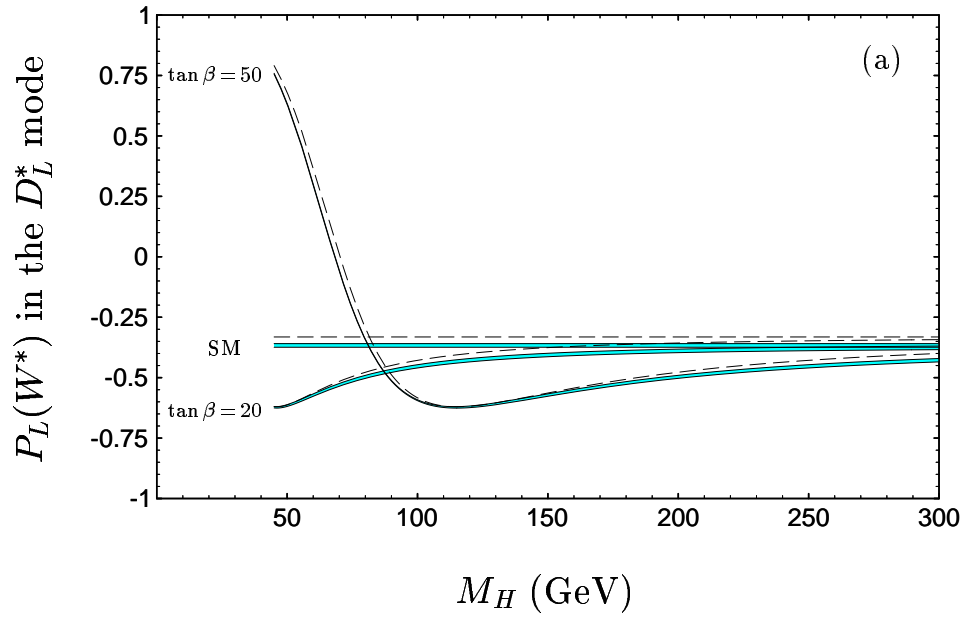


Fig. 5